The jaw is a second-class lever in *Pedetes capensis* (Rodentia: Pedetidae)

Philip G Cox Corresp. 1, 2

1 Department of Archaeology, University of York, York, UK
2 Hull York Medical School, University of York, York, UK

Corresponding Author: Philip G Cox
Email address: philip.cox@hyms.ac.uk

The mammalian jaw is often modelled as a third-class lever for the purposes of biomechanical analyses, owing to the position of the resultant muscle force between the jaw joint and the teeth. However, it has been proposed that in many rodents, the jaws operate as a second-class lever during distal molar bites, owing to the rostral position of the masticatory musculature. In particular, the infraorbital portion of the zygomatico-mandibularis (IOZM) has been suggested to be of major importance in converting the masticatory system from a third-class to a second-class lever. The presence of the IOZM is diagnostic of the hystricomorph rodents, and is particularly well-developed in *Pedetes capensis*, the South African springhare. In this study, finite element analysis (FEA) was used to assess the lever mechanics of the springhare masticatory system, and to determine the function of the IOZM. An FE model of the skull of *P. capensis* was constructed and loaded with all masticatory muscles, and then solved for biting at each tooth in turn. Further load cases were created in which each masticatory muscle was removed in turn. The analyses showed that the mechanical advantage of the springhare jaws was above one at all molar bites and very close to one during the premolar bite. Removing the IOZM or masseter caused a drop in mechanical advantage at all bites, but affected strain patterns and cranial deformation very little. Removing the ZM had only a small effect on mechanical advantage, but produced a substantial reduction in strain and deformation across the skull. It was concluded that the masticatory system of *P. capensis* acts as a second class lever during bites along almost the entire cheek tooth row. The IOZM is clearly a major contributor to this effect, but the masseter also has part to play. The benefit of the IOZM is that it adds force without substantially contributing to strain or deformation of the skull. This may help explain why the hystricomorphous morphology has evolved multiple times independently within Rodentia.

The jaw is a second-class lever in *Pedetes capensis* (Rodentia: Pedetidae)

Philip G. Cox[1,2]

[1]Department of Archaeology, University of York, York, YO10 5DD, UK

[2]Hull York Medical School, University of York, York, YO10 5DD, UK

Corresponding author:

Philip G. Cox

Email: philip.cox@hyms.ac.uk

ABSTRACT

The mammalian jaw is often modelled as a third-class lever for the purposes of biomechanical analyses, owing to the position of the resultant muscle force between the jaw joint and the teeth. However, it has been proposed that in many rodents, the jaws operate as a second-class lever during distal molar bites, owing to the rostral position of the masticatory musculature. In particular, the infraorbital portion of the zygomatico-mandibularis (IOZM) has been suggested to be of major importance in converting the masticatory system from a third-class to a second-class lever. The presence of the IOZM is diagnostic of the hystricomorph rodents, and is particularly well-developed in *Pedetes capensis*, the South African springhare. In this study, finite element analysis (FEA) was used to assess the lever mechanics of the springhare masticatory system, and to determine the function of the IOZM. An FE model of the skull of *P. capensis* was constructed and loaded with all masticatory muscles, and then solved for biting at each tooth in turn. Further load cases were created in which each masticatory muscle was removed in turn. The analyses showed that the mechanical advantage of the springhare jaws was above one at all molar bites and very close to one during the premolar bite. Removing the IOZM or masseter caused a drop in mechanical advantage at all bites, but affected strain patterns and cranial deformation very little. Removing the ZM had only a small effect on mechanical advantage, but produced a substantial reduction in strain and deformation across the skull. It was concluded that the masticatory system of *P. capensis* acts as a second class lever during bites along almost the entire cheek tooth row. The IOZM is clearly a major contributor to this effect, but the masseter also has part to play. The benefit of the IOZM is that it adds force without substantially contributing to strain or deformation of the skull. This may help explain why the hystricomorphous morphology has evolved multiple times independently within Rodentia.

INTRODUCTION

The mammalian jaw is frequently treated as a lever for the purposes of biomechanical analysis (e.g. Crompton, 1963; Greaves, 1978; Thomason, 1991; Davis et al., 2010). More specifically, it is frequently considered to be a third-class lever i.e. one in which the input force sits between the fulcrum and the output force (Kerr, 2010). In mammals, the resultant masticatory muscle force (the input force) is usually situated between the jaw joint (fulcrum) and the biting tooth (output force) and thus the comparison with a third-class lever is generally accurate. The advantage of positioning muscle force posterior to the teeth is that relatively wide gapes can be achieved and high tensile forces at the jaw joint are avoided (Greaves, 2012). However, the trade-off is that the mechanical advantage of a third-class lever is always less than one – that is, the output bite force will always be less than the input muscle force.

A number of authors have proposed that mammalian jaws do not always operate as third-class levers (Davis, 1955; Turnbull, 1970), and can in certain circumstances act as second-class levers with the output force between fulcrum and input force. In many rodents (and also in a few ungulates), it has been suggested that the relative size and position of the masseter can the resultant of the masticatory musculature anterior to the distal cheek teeth, converting the masticatory system into a second-class lever during distal molar biting (Turnbull, 1970; Samuels, 2009). Such an effect has even been claimed to occur in humans, with the jaw operating as a second-class lever during bites on the second and third molars (Mansour & Reynik, 1975). Alternatively, other authors have argued that although some parts of the muscle mass attach far forward on the jaws in rodents, the resultant muscle force is still located towards the posterior end of the jaw (Greaves, 2012).

In rodents, one muscle in particular has been identified as contributing to the jaw operating as a second-class lever. The infraorbital portion of the zygomatico-mandibularis (IOZM) is an anterior expansion of the deepest layer of the masseter, the zygomatico-mandibularis (ZM), which passes through the enlarged infraorbital foramen to take its origin on the lateral surface of the rostrum. The IOZM, also referred to as the maxillo-mandibularis (Becht, 1953; Turnbull, 1970) or medial masseter (Wood, 1965; Woods, 1972), is the one of the defining characters of hystricomorph rodents, but is also present in a somewhat smaller form in myomorphs, where it is

found in combination with a rostral expansion of the deep masseter (Wood, 1965; Cox & Jeffery, 2011). Given its rostral origin on the skull and its mandibular insertion at the level of the premolar, Becht (1953) believed the function of the IOZM was to convert the jaw from a third-class lever to a second-class lever during molar biting.

This study seeks to understand the lever mechanics of the skull in the South African springhare, *Pedetes capensis* – a rodent species in which the IOZM is notably well-developed (Offermans & De Vree, 1989). *P. capensis* is a nocturnal, bipedal, saltatorial rodent that inhabits arid and semi-arid areas of southern Africa (Peinke & Brown, 2003). It is large for a rodent (3-4 kg) and feeds principally on grasses, especially the rhizomes of *Cynodon dactylon* and the tubers of *Cyperus esculentus* (Peinke & Brown, 2006). *P. capensis* and its sister-species *P. surdaster* are the only two extant members of the Pedetidae (Wilson & Reeder, 2005), a family which molecular analyses place as sister-group to the Anomaluridae (scaly-tailed flying squirrels) in the Anomaluromorpha, which itself is part of the mouse-related clade (Fabre et al., 2012). Given the presence of the IOZM muscle, the pedetids (and anomalurids) have been identified as being hystricomorphous (Wood, 1965). However, the hystricomorphy seen in the Anomaluromorpha has evolved independently from that seen in three other groups of rodents: the Ctenohystrica, the Dipodidae, and some members of the Gliridae (Hautier, Cox & Lebrun, 2015). Thus, the function of the IOZM is of prime interest to understanding the evolution of the rodents – why has this muscle arisen independently so many times throughout rodents?

The aim of this study is to model the masticatory system of *P. capensis* to determine if it functions as a second or third-class lever, and to assess the function of the masticatory muscles, particularly the IOZM. There are two specific hypotheses that will be tested:

1. It is hypothesised that a model of the skull of *P. capensis* will demonstrate the masticatory system operating as a second-class lever along most of the molar tooth row. This is expected based on previous dissection work by Offermans and De Vree (1989) who showed that a great deal of the masticatory musculature is situated alongside or anterior to the cheek teeth. The masticatory system will be determined to be a second-class lever when the bite force exceeds the resultant input muscle force, i.e. when the

mechanical advantage is greater than one, and when the reaction force at the temporo-mandibular joint is negative.

2. It is hypothesised that the IOZM muscle has a major role in converting the masticatory system from a third to a second-class lever in *P. capensis*. This hypothesis was previously proposed by Becht (1953) and is also expected owing to the large size and rostral position of the IOZM (Offermans & De Vree, 1989, 1993). The function of the IOZM will be determined by virtual ablation analyses i.e. removing it and other muscles from the models to elucidate the effect on the biomechanical performance of the system, as determined by mechanical advantage, principal strains and the overall deformation of the skull during biting.

To address these hypotheses and to study the function of the springhare skull during biting, finite element analysis (FEA) will be employed. FEA is an engineering technique for predicting stress, strain and deformation in an object during loading (Rayfield, 2011), and is now frequently applied to reconstructions of skulls and other skeletal elements in order to analyse vertebrate biomechanics (e.g. Dumont et al., 2011; Cox et al., 2012; Cox, Kirkham & Herrel, 2013; O'Hare et al., 2013; Figueirido et al., 2014; Sharp, 2015; McIntosh & Cox, 2016; McCabe et al., 2017). As well as simulating stress and strain distributions, FEA is also able to predict reaction forces, and so will be used here to determine bite force, jaw joint reaction force and mechanical advantage. Although these metrics could in theory be estimated via simple 2D lever models, it has been shown that such simplification leads to inaccuracies in muscle attachment areas, force magnitudes and directions of pull (Davis et al., 2010; Greaves, 2012). The advantage of FEA is that muscle forces can be distributed across the whole attachment site rather than being modelled as originating from a single centroid point, and muscle force vectors can act in three dimensions rather than two.

MATERIALS AND METHODS

Sample and model creation

A cranium and mandible of *Pedetes capensis*, the South African springhare, were obtained from the University Museum of Zoology, Cambridge (catalogue number E.1446) and microCT scanned on the X-Tek Metris system in the Medical and Biological Engineering group,

University of Hull. Voxels were isometric with dimensions of 0.052 mm and 0.041 mm for the cranium and mandible respectively.

A virtual reconstruction of the cranium was created from the scan using Avizo 8 (FEI, Hillsboro, OR). Bone and teeth were segmented as separate materials, but no differentiation was made between cortical and trabecular bone, nor between different materials within the teeth. These simplifications of the model geometry were felt to be justified as several previous studies have indicated that, whilst absolute strain magnitudes are impacted by the presence or absence of trabecular bone and different tooth materials, the large-scale patterns of deformation are relatively insensitive to such changes (Fitton et al., 2015; Toro-Ibacache et al., 2016). The cranial reconstruction was then converted into an eight-noded, cubic finite element (FE) mesh via direct voxel conversion, implemented in VOX-FE, custom-built open-source FE software (Liu et al., 2012). The Avizo reconstruction and VOX-FE model are both available for download at https://figshare.com/articles/Springhare_FEA/5082598.

Material properties, constraints and loads

Material properties were assigned to the model based on previous nano-indentation work on rodent skulls (Cox et al., 2012). Both bone and teeth were assumed to be linearly elastic isotropic with Young's moduli of 17 and 30 GPa respectively and a Poisson's ratio of 0.3 for both. The model was constrained at both temporo-mandibular joints as well as the biting tooth. As in previous rodent FE models (Cox, Kirkham & Herrel, 2013; Cox, Rinderknecht & Blanco, 2015; McIntosh & Cox, 2016), the jaw joints were constrained in all three dimensions, whilst the bite points were only constrained in the bite direction (i.e. orthogonal to the occlusal plane). The number of nodes constrained at each location varied between 158 and 332.

Loads were applied to both sides of the model to simulate the following jaw-closing muscles: masseter (combining the superficial and deep layers), posterior masseter, ZM, IOZM, temporalis, medial pterygoid and lateral pterygoid. Muscle attachment sites were determined based on the detailed descriptions and figures in Offermans & De Vree (1989). Muscle directions of pull were assigned using landmarks recorded from the insertion areas on a reconstruction of the springhare mandible, created from the previously gathered microCT scans. Muscle forces were calculated

by multiplying the physiological cross-sectional areas (PCSA) given in Offermans & De Vree (1993) by an intrinsic muscle stress value of 0.3 Nmm^{-2} (van Spronsen et al., 1989). These muscle forces were then modified based on the maximum percentage activations recorded by electromyography during incision and mastication of groundnuts (Offermans & DeVree, 1993). Thus the relative proportions of total muscle force provided by each muscle were different in incisor biting to premolar/molar biting. Applied muscle forces for incision and mastication are given in Table 1. In order to ascertain the function of the masticatory muscles, versions of the model were created without each of the muscles in turn. The loaded FE model is shown in Figure 1.

Model solution and analysis

The model was solved for biting at each tooth along the dental arcade. Based on experimental work by Offermans & De Vree (1990), all bites were modelled as bilateral. Reaction forces at the biting tooth and at the jaw joints were calculated for each loadcase. Bite forces were divided by the resultant input muscle force (equal to the sum of the bite force and joint reaction forces) to calculate the mechanical advantage of the masticatory system at each tooth. As a ratio, the mechanical advantage provides a useful metric for comparing loadcases with different input muscle forces. It should be noted that it is a different measure to the mechanical efficiency of biting used in other studies (Dumont et al, 2011; Cox et al, 2012; Cox, Kirkham & Herrel, 2013), which divides the bite force by the total adductor muscle force, but does not take into account the orientation of muscle vectors. The distribution of maximum (ε_1: predominantly tensile) and minimum (ε_3: predominantly compressive) principal strains across the skull were examined using contour maps. Geometric morphometric methods were used to analyse deformation patterns across the skull (Cox et al., 2011; Cox, Kirkham & Herrel, 2013; O'Higgins et al., 2011; McIntosh & Cox, 2016). A set of 46 3D landmark co-ordinates (described in Figure 2 and Table S1), based on that used in Cox, Kirkham & Herrel (2013), was recorded from each solved model as well as from the original unloaded model. As changes in size are of equal significance to changes in shape during mechanical loading, the landmark sets were subjected to a Procrustes size and shape analysis (O'Higgins & Milne, 2013), not a Procrustes form analysis, which gives a lower weighting to size (Fitton et al., 2015). This was followed by a principal component

analysis (PCA). All analyses were implemented in the EVAN toolbox software (www.evan-society.org).

RESULTS

The absolute bite forces and joint reaction forces predicted during biting at each tooth in *P. capensis* are given in Table 2. In addition, the mechanical advantage of the jaws at each bite has been calculated. It can be seen that joint reaction forces are negative and mechanical advantage exceeds one at all three molar teeth. In addition, the mechanical advantage is almost one (0.99) and the joint reaction force is close to zero (2.8 N) at the premolar.

The effect of removing each of the masticatory muscles on the mechanical advantage is given in Table 2 and shown in Figure 3. Removal of either the IOZM or the masseter causes a decrease in mechanical advantage during both incision and mastication, with removal of the IOZM leading to the greatest decrease. Removal of the medial pterygoid muscle leads to an increase in mechanical advantage across all cheek teeth, but little effect is seen during incisor biting. Removal of the ZM causes a substantial drop in bite force at all teeth, but has little effect on the mechanical advantage of the system, except at the incisor where mechanical advantage increases in the absence of the ZM. Removal of the posterior masseter, temporalis or lateral pterygoid results in very little change in either bite force or mechanical advantage at any of the teeth, and hence the results of the models lacking these muscles have not been illustrated in Figure 3.

The contour maps of principal strain distribution across the cranium of *P. capensis* during biting on the incisor and first molar are shown in Figure 4. It can be seen that the highest maximum and minimum principal strains are concentrated in similar areas of the skull – along the zygomatic arch and up its wide ascending ramus, and across the orbital wall, especially the anterior part. However, there are some differences between the strain distributions. The ascending ramus of the zygomatic arch is subject to greater ε_1 strains than ε_3 strains, and thus is predominantly under tension, whereas the orbital wall seems to be experiencing greater ε_3 strains and is likely mostly in compression. Strains are generally greater during molar biting than incision, and there is an overall caudal shift of the most highly strained regions away from the rostrum towards the orbit as the bite point moves posteriorly along the tooth row.

247

248 Figure 4 also shows the effect of removing three of the masticatory muscles (IOZM, masseter
249 and ZM) on principal strain distributions. Despite being relatively large muscles, the impact of
250 removing the IOZM or the masseter is minimal. There are very few differences between models
251 with all masticatory muscles applied and those without the IOZM, except for a slight reduction in
252 strain in the posterior part of the orbit during incisor and molar biting. Removal of the masseter
253 has little effect on the strains generated by incisor biting, but reduces strains across the
254 zygomatic arch and in the anterior part of the orbit during molar biting. Elimination of the ZM
255 from the model, however, leads to a substantial reduction in ε_1 and ε_3 strains across the skull
256 during bites at all teeth.

257

258 The geometric morphometric analysis highlights differences in the magnitude and mode of
259 deformation between the different loadcases solved in this study. Figure 5 shows the scatter plot
260 of the first two principal components. The first principal component encompasses 90% of the
261 variation, and the second principal component 9% of the variation. It should be noted that to be
262 able to visualise change across PC2, the axes have not been shown to the same scale. As
263 demonstrated by the warped reconstructions in Figure 5, the shape change along PC1 is mainly
264 bending of the zygomatic arch, and this axis mostly separates loaded models from the unloaded
265 skull, incisor bites from bites on other teeth, and models with different muscles excluded from
266 one another. In general, incisor bites result in smaller deformations than cheek tooth bites (that
267 is, the incisor bites are found closer to the unloaded model on PC1), whereas premolar and molar
268 bites produce very similar deformations. Models lacking the IOZM, temporalis, medial pterygoid
269 or lateral pterygoid deform in a very similar manner to the models with all masticatory muscles,
270 whereas removal of the posterior masseter reduces the magnitude of deformation very slightly.
271 Removal of the masseter causes a greater reduction in cranial deformation and elimination of the
272 ZM (the largest masticatory muscle) causes the largest reduction in deformation. Shape change
273 along PC2 represents dorso-ventral bending of the skull and separates the four different bites
274 along the cheek tooth row.

275

276

277

DISCUSSION

The results of this study support both of the hypotheses proposed here. The skull of *Pedetes capensis* operates as a second-class lever during biting along almost all of the cheek teeth (first hypothesis), and this effect can be largely ascribed to the presence of the IOZM muscle (second hypothesis), although the masseter is important in this regard as well.

Second-class vs third class lever

The FE model of *P. capensis* indicates that the mechanical advantage of the masticatory system is greater than one and the reaction forces at the temporo-mandibular joints are negative during bites on all three molars. Furthermore, the mechanical advantage is almost one and the joint reaction force is very close to zero during premolar biting. Thus, as the bite point moves distally along the tooth row, the system switches from a third-class to a second-class lever somewhere between the premolar and first molar. This effect may be driven in large part by the unusual cranial morphology of the springhare. In most hystricomorph rodents, the anterior root of the zygomatic arch arises from the skull approximately at the level of the first cheek tooth, but in *P. capensis* it is much further forward, attaching to the shortened rostrum just posterior to the maxillary incisor (Offermans & De Vree, 1989). Thus, the masticatory musculature, as a whole, is more rostrally positioned than in most other rodents, and so the jaw becomes a second-class lever at more anterior position along the tooth row.

The impact of this morphological arrangement is that the springhare is able to generate very high bite forces (between 350 and 550 N) at its molar teeth. Moreover, these bites are efficient – as a second-class lever, the generated bite force is greater than the input resultant muscle force – so high bite forces can be produced without having to massively increase the overall adductor muscle mass. It is likely that *P. capensis* has evolved this highly efficient feeding system in order to cope with the demands of the arid environment in which it lives (Peinke & Brown, 2003). Springhares are herbivorous, feeding almost exclusively on grasses (Peinke & Brown, 2006). Although they are known to eat the leaves, springhares tend to favour underground storage organs, such as rhizomes and tubers, particularly during autumn and winter when nutritional reserves are transferred away from leaves and into the leaf bases and roots (Peinke & Brown, 2006). These storage organs tend to be mechanically demanding to eat, requiring a great deal of

mastication to break down, which may have driven the evolution of the highly efficient masticatory system of springhares. The disadvantage of the masticatory arrangement seen in *P. capensis* is that the rostral position of many of the jaw-closing muscles is likely to severely limit maximum gape. However, given their preferred diet of grasses, these limitations are not likely to impact the ability of springhares to feed effectively.

Function of the masticatory muscles

The virtual ablation experiments, in which masticatory muscles were sequentially removed from the FE model, show that the IOZM is the most important muscle in converting the masticatory system from a third-class to second-class lever, as predicted by the second hypothesis. When the IOZM is removed, the mechanical advantage decreases, indicating that more force is being directed towards the jaw joints. This has the effect that the point at which the system switched from operating as a third-class to a second-class lever moves back to somewhere between the first and second molars. Thus, this result supports the idea proposed by Becht (1953) that the function of the IOZM is to convert the masticatory system to a second-class lever during molar biting, at least in *P. capensis*. Removal of the IOZM had very little impact on the distribution and magnitudes of strain across the skull (Figure 4), nor did it greatly change the overall deformation of the skull during biting (Figure 5), as has also been noted in another species of rodent, *Laonastes aenigmamus* (Cox, Kirkham & Herrel, 2013). Thus, it appears that the increase in mechanical advantage gained by the presence of an IOZM muscle does not come at the cost of increased strain or deformation, either in the region of the IOZM origin or elsewhere on the skull.

The ZM is one of the largest masticatory muscles in the springhare (Offermans & DeVree, 1993), but its removal from the FE model had very little effect on the efficiency of the masticatory system i.e. the mechanical advantage and joint reaction force remained largely the same. Thus, by virtue of being large, the ZM is an important muscle for increasing overall bite force, but its presence does not alter the efficiency of the system a great deal. However, the ZM does have a large effect on the deformation of the springhare skull during biting. The GMM analysis showed that elimination of the ZM greatly reduces the magnitude of deformation experienced by the skull (Figure 5), much more so than any other masticatory muscle. This

appears to be a consequence of the attachment site of the ZM on the zygomatic arch. As has been found in other FEA studies of mammal skulls (Bright, 2012; Cox et al., 2012; Fitton et al., 2012), the morphology of the zygomatic arch makes it susceptible to larger deformations than other parts of the skull. Indeed, in this study, deformations of the zygoma overwhelm deformations in all other parts of the skull, as can be seen from the warped reconstructions in Figure 5. The large size and location of the ZM in *P. capensis* leads to it being the principal generator of zygomatic strain and deformation. This can be seen in Figure 4, where removal of the ZM vastly reduces strain in the zygomatic arch.

It has been suggested that the large zygomatic strains seen in many FEA studies of mammalian skulls may be artificial and the result of a failure to incorporate important soft tissue structures into the models. In particular, the temporal fascia has been shown to resist inferior bending of the zygomatic arch in an FE model of a macaque (Curtis et al., 2011). This is unlikely to be the case here as no temporal fascia was reported by Offermans & De Vree (1989) in their dissection of a springhare. Furthermore, the temporalis is extremely small in *P. capensis*, and the temporal region is positioned distinctly caudal the zygomatic arch, which would reduce the ability of a temporal fascia to counteract ventral deflection of the zygomatic arch. However, there is an aponeurosis attached extensively around the margin of the infraorbital fossa (Offermans & De Vree, 1989), which may have the potential to resist some bending in the anterior part of the zygomatic arc and its ascending ramus. Further work, both *ex vivo* dissection and *in silico* modelling, is necessary to understand the biomechanical consequence of this aponeurosis.

The masseter has been shown to have a similar effect to the IOZM with regard to bite force, although not quite to the same extent. It, too, appears to shift the resultant masticatory muscle force anteriorly along the rostrum, thus directing force towards the biting tooth and away from the jaw joints. Removal of the masseter has much the same effect as removing the IOZM – the mechanical advantage is decreased and the point at which the system becomes a second-class lever is shifted posteriorly along the tooth row. Unfortunately for this study, Offermans & DeVree (1993) did not separate the superficial and deep masseter when measuring PCSA, so the two muscles could not be modelled separately in the FEA. However, the illustrations in Offermans & DeVree (1989) indicate that the fibres of the superficial masseter have a more

horizontal alignment than those of the deep masseter (as in most rodents, e.g. Turnbull, 1970), so it is likely that the superficial masseter is the more important division of the masseter with regard to the operation of the jaw as a second-class lever. In terms of cranial deformations, the masseter has a similar, but lesser, effect to the ZM. Owing to its attachment to the zygomatic arch, the action of the masseter generates inferior bending of the arch, and thus its removal tends to reduce global deformation of the springhare cranium (Figure 5). It can also be seen that that removal of the masseter causes a slight reduction in zygomatic and orbital strains during molar biting (Figure 4).

The medial pterygoid, because of its posterior line of action, tends to direct muscle force away from the teeth and towards the jaw joints, unlike the IOZM and masseter. Thus removal of the medial pterygoid increased the mechanical advantage of the masticatory system. Overall, the presence of the medial pterygoid increases bite force because it increases the total input adductor muscle force, but it does so in a somewhat inefficient manner. However, it has been shown that the medial pterygoid is important in other aspects of masticatory biomechanics, notably as a counterbalance to the lateral pull of the masseter, thereby preventing wishboning of the mandible (eversion of the lower border and angular process) and reducing tensile strains at the symphysis (Hiiemae, 1971; Satoh, 1998; Cox & Jeffery, 2015).

The posterior masseter, temporalis and lateral pterygoid are very small compared to the other masticatory muscles in *P. capensis*, each providing less than 11% of the total adductor muscle force. Hence, the impact of their removal on bite force and mechanical advantage was minimal. Similarly, removal of these muscles had a very limited impact on the overall deformation of the skull (Figure 5). The models without the temporalis and lateral pterygoid can barely be distinguished from the models with all masticatory muscles. The models without a posterior masseter show a very slight reduction in the magnitude of cranial deformation. This is because the posterior masseter attaches to the caudal part of the zygomatic arch and thus is able to cause a small amount of posterior deflection. It is likely that these muscles contribute to aspects of the masticatory process other than bite force generation, especially the antero-posterior movements of the mandible relative to the skull that are common to rodents. The temporalis, whilst clearly too small to be a powerful elevator of the jaw as in myomorphs (Hiiemae, 1971; Gorniak, 1977),

may have a braking role during the power stroke of chewing (Byrd, 1981), and the lateral pterygoid may be important in protraction of the mandible (Weijs & Dantuma, 1975; Gorniak, 1977).

CONCLUSIONS

The masticatory system of *P. capensis* has been shown to act as a second-class lever along the majority of the cheek tooth row and, as predicted by Becht (1953), the IOZM is a particularly important muscle in the switch from third-class to second-class lever mechanics. It should be noted that masseter also plays an important role in this regard. This analysis of muscle function is, of course, specific to *P. capensis* and further analyses of other species are necessary to determine whether the conclusions hold true for other rodents. However, the position of the IOZM, far forward on the rostrum, makes it likely that it will have some role to play in increasing the mechanical advantage of the masticatory system in most hystricomorph rodents (the exact scale of the effect being dependent on the size of the IOZM relative to the other masticatory muscles). Previous research has suggested that, amongst rodents, sciuromorphs are adapted for efficient gnawing at the incisors, whereas hystricomorphs are adapted to efficient grinding at the molars (Cox et al, 2012). Druzinsky (2010) determined that of all the masticatory muscles, it is the anterior deep masseter that confers efficacious incisor bites in sciuromorphs. Here, it is indicated that the IOZM provides efficiency in molar bites in hystricomorphs, without substantially increasing strains across the skull or the magnitude of cranial deformation. This may go some way to explaining why hystricomorphy has evolved convergently at least four times within the rodents.

ACKNOWLEDGEMENTS

The author thanks Matt Lowe and Rob Asher (University Museum of Zoology, Cambridge) for the loan of the specimen, and Sue Taft and Michael Fagan (Medical and Biological Engineering Group, University of Hull) for microCT scanning. Thanks are due to Paul O'Higgins for help with geometric morphometrics.

REFERENCES

Becht G. 1953. Comparative biologic-anatomical researcher on mastication in some mammals. *Proceedings of the Koninklijke Nederlandse Akademie van Wetenschappen. Series C* **56:** 508-526.

Bright JA. 2012. The importance of craniofacial sutures in biomechanical finite element models of the domestic pig. *PLoS ONE* **7:** e31769.

Byrd KE. 1981. Mandibular movement and muscle activity during mastication in the guinea pig (*Cavia porcellus*). *Journal of Morphology* **170:** 147-169.

Cox PG, Fagan MJ, Rayfield EJ, Jeffery N. 2011. Finite element modelling of squirrel, guinea pig and rat skulls: using geometric morphometrics to assess sensitivity. *Journal of Anatomy* **219:** 696-709.

Cox PG, Jeffery N. 2011. Reviewing the jaw-closing musculature in squirrels, rats and guinea pigs with contrast-enhanced microCT. *Anatomical Record* **294:** 915-928.

Cox PG, Jeffery N. 2015. The muscles of mastication and the function of the medial pterygoid. In: Cox PG, Hautier L, eds. *Evolution of the Rodents: Advances in Phylogeny, Functional Morphology and Development.* Cambridge: Cambridge University Press, 350-372.

Cox PG, Kirkham J, Herrel A. 2013. Masticatory biomechanics of the Laotian rock rat, *Laonastes aenigmamus*, and the function of the zygomaticomandibularis muscle. *PeerJ* **1:** e160.

Cox PG, Rayfield EJ, Fagan MJ, Herrel A, Pataky TC, Jeffery N. 2012. Functional evolution of the feeding system in rodents. *PLoS ONE* **7:** e36299.

Cox PG, Rinderknecht A, Blanco RE. 2015. Predicting bite force and cranial biomechanics in the largest fossil rodent using finite element analysis. *Journal of Anatomy* **226:** 215-223.

Crompton AW. 1963. The evolution of the mammalian jaw. *Evolution* **17:** 431-439.

Curtis N, Witzel U, Fitton LC, O'Higgins P, Fagan MJ. 2011. The mechanical significance of the temporal fasciae in *Macaca fascicularis*: an investigation using finite element analysis. *Anatomical Record* **294:** 1178-1190.

Davis DD. 1955. Masticatory apparatus in the spectacled bear *Tremarctos ornatus*. *Fieldiana (Zoology)* **37:** 25-46.

462 **Davis JL, Santana SE, Dumont ER, Grosse IR. 2010.** Predicting bite force in mammals: two-
463 dimensional *versus* three-dimensional lever models. *Journal of Experimental Biology*
464 **213:** 1844-1851.
465 **Druzinsky RE. 2010.** Functional anatomy of incisal biting in *Aplondontia rufa* and sciuromorph
466 rodents – Part 2: Sciuromorphy is efficacious for production of force at the incisors. *Cells*
467 *Tissues Organs* **192:** 50-63.
468 **Dumont ER, Davis JL, Grosse IR, Burrows AM. 2011.** Finite element analysis of performance
469 in the skulls of marmosets and tamarins. *Journal of Anatomy* **218:** 151-162.
470 **Fabre P-H, Hautier L, Dimitrov D, Douzery EJP. 2012.** A glimpse on the pattern of rodent
471 diversification: a phylogenetic approach. *BMC Evolutionary Biology* **12:** 88.
472 **Figueirido B, Tseng JZ, Serrano-Alarcón FJ, Martín-Serra A, Pastor JF. 2014.** Three-
473 dimensional computer simulations of feeding behaviour in red and giant pandas relate
474 skull biomechanics with dietary niche partitioning. *Biology Letters* **10:** 20140196.
475 **Fitton LC, Shi JF, Fagan MJ, O'Higgins P. 2012.** Masticatory loadings and cranial
476 deformation in *Macaca fascicularis*: a finite element analysis sensitivity study. *Journal of*
477 *Anatomy* **221:** 55-68.
478 **Fitton LC, Proa M, Rowland C, Toro-Ibacache V, O'Higgins P. 2015.** The impact of
479 simplifications on the performance of a finite element model of a *Macaca fascicularis*
480 cranium. *Anatomical Record* **298:** 107-121.
481 **Gorniak GC. 1977.** Feeding in golden hamsters, *Mesocricetus auratus*. *Journal of Morphology*
482 **154:** 427-458.
483 **Greaves WS, 1978.** The jaw lever system in ungulates: a new model. *Journal of Zoology* **184:**
484 271-285.
485 **Greaves WS. 2012.** *The Mammalian Jaw: A Mechanical Analysis*. Cambridge: Cambridge
486 University Press.
487 **Hautier L, Cox PG, Lebrun R. 2015.** Grades and clades among rodents: the promise of
488 geometric morphometrics. In: Cox PG, Hautier L, eds. *Evolution of the Rodents:*
489 *Advances in Phylogeny, Functional Morphology and Development.* Cambridge:
490 Cambridge University Press, 277-299.

Hiiemae K. 1971. The structure and function of the jaw muscles in the rat (*Rattus norvegicus* L.) III. The mechanics of the muscles. *Zoological Journal of the Linnean Society* **50:** 111-132.

Kerr A. 2010. *Introductory Biomechanics*. Edinburgh: Churchill Livingstone.

Liu J, Shi L, Fitton LC, Phillips R, O'Higgins P, Fagan MJ. 2012. The application of muscle wrapping to voxel-based finite element models of skeletal structures. *Biomechanics and Modeling in Mechanobiology* **11:** 35-47.

Mansour RM, Reynik RJ. 1975. *In vivo* occlusal forces and moments: I. Forces measured in terminal hinge position and associated moments. *Journal of Dental Research* **54:** 114-120.

McCabe K, Henderson K, Pantinople J, Richards HL, Milne N. 2017. Curvature reduces bending strains in the quokka femur. *PeerJ* **5:** e3100.

McIntosh AF, Cox PG. 2016. The impact of gape on the performance of the skull in chisel-tooth digging and scratch digging mole-rats (Rodentia: Bathyergidae). *Royal Society Open Science* **3:** 160568.

Offermans M, De Vree F. 1989. Morphology of the masticatory apparatus in the springhare, *Pedetes capensis*. *Journal of Mammalogy* **70:** 701-711.

Offermans M, De Vree F. 1990. Mastication in springhares, *Pedetes capensis*: A cineradiographic study. *Journal of Morphology* **205 :** 353-367.

Offermans M, De Vree F. 1993. Electromyography and mechanics of mastication in the springhare *Pedetes capensis* (Rodentia, Pedetidae). *Belgian Journal of Zoology* **123:** 231-261.

O'Hare LMS, Cox PG, Jeffery N, Singer ER. 2013. Finite element analysis of stress in the equine proximal phalanx. *Equine Veterinary Journal* **45:** 273-277.

O'Higgins P, Cobb SN, Fitton LC, Gröning F, Phillips R, Liu J, Fagan MJ. 2011. Combining geometric morphometrics and functional simulation: an emerging toolkit for virtual functional analyses. *Journal of Anatomy* **218:** 3-15.

O'Higgins P, Milne N. 2013. Applying geometric morphometrics to compare changes in size and shape arising from finite elements analysis. *Hystrix* **24:** 126-132.

Peinke DM, Brown CR. 2003. Metabolism and thermoregulation in the springhare (*Pedetes capensis*). *Journal of Comparative Physiology B* **173:** 347-353.

Peinke DM, Brown CR. 2006. Habitat use by the southern springhare (*Pedetes capensis*) in the Eastern Cape Province, South Africa. *South African Journal of Wildlife Research* **36:** 103-111.

Rayfield EJ. 2007. Finite element analysis and understanding the biomechanics and evolution of living and fossil organisms. *Annual Review of Earth and Planetary Science* **35:** 541-576.

Samuels JX. 2009. Cranial morphology and dietary habits of rodents. *Zoological Journal of the Linnean Society* **156:** 864-888.

Satoh K. 1998. Balancing function of the masticatory muscles during incisal biting in two murid rodents, *Apodemus speciosus* and *Clethrionomys rufocanus*. *Journal of Morphology* **236:** 49-56.

Sharp A. 2015. Comparative finite element analysis of the cranial performance of four herbivorous marsupials. *Journal of Morphology* **276:** 1230-1243.

Thomason JJ, 1991. Cranial strength in relation to estimated biting forces in some mammals. *Canadian Journal of Zoology* **69:** 2326-2333.

Toro-Ibacache V, Fitton LC, Fagan MJ, O'Higgins P. 2016. Validity and sensitivity of a human cranial finite element model: implications for comparative studies of biting performance. *Journal of Anatomy* **228:** 70-84.

Turnbull WD. 1970. Mammalian masticatory apparatus. *Fieldiana (Geology)* **18:** 147-356.

van Spronsen PH, Weijs WA, Valk J, Prahl-Andersen B, van Ginkel FC. 1989. Comparison of jaw-muscle bite-force cross-sections obtained by means of magnetic resonance imaging and high-resolution CT scanning. *Journal of Dental Research* **68:** 1765-1770.

Weijs WA, Dantuma R. 1975. Electromyography and mechanics of mastication in the albino rat. *Journal of Morphology* **146:** 1-34.

Wilson DE, Reeder DM. 2005. *Mammal Species of the World*. Baltimore: Johns Hopkins Press.

Wood AE. 1965. Grades and clades among rodents. *Evolution* **19:** 115-130.

Woods CA. 1972. Comparative myology of jaw, hyoid and pectoral appendicular regions of New and Old World hystricomorph rodents. *Bulletin of the American Museum of Natural History* **147:** 115-198.

553 **FIGURE LEGENDS**

554 **Figure 1. FE model showing muscle attachment sites and vectors.** Skull of *Pedetes capensis*
555 shown in (A) lateral and (B) dorso-lateral view. Key: light green, IOZM; yellow, lateral
556 pterygoid; blue, masseter; orange, medial pterygoid; brown, posterior masseter; red,
557 temporalis; dark green, zygomaticomandibularis.
558
559 **Figure 2. Landmarks used in GMM analysis of skull deformations.** Reconstruction of skull
560 of *Pedetes capensis* in (A) dorsal, (B) ventral and (C) left lateral view. Landmarks 11-28
561 recorded on both sides of the skull. Landmark descriptions are given in Table S1.
562
563 **Figure 3. Mechanical advantage at each tooth predicted by FE model.** Abbreviations: I,
564 incisor; PM, premolar; M1, first molar; M2, second molar; M3, third molar. Key: purple
565 line with circle, model with all muscles; blue line with crosses, masseter removed; light
566 green line with diamonds, IOZM removed; dark green line with triangles, ZM removed;
567 orange line with squares, medial pterygoid removed. Models with posterior masseter,
568 temporalis and lateral pterygoid removed not shown.
569
570 **Figure 4. Predicted principal strains across the skull of *Pedetes capensis* during incisor and**
571 **first molar biting.** Left, maximum (ε_1) principal strain; right, minimum (ε_3) principal
572 strains. First line, model with all masticatory muscles included; second line, model with
573 IOZM excluded; third line, model with masseter excluded; fourth line, model with ZM
574 excluded.
575
576 **Figure 5. GM analysis of cranial deformations in *Pedetes capensis*.** Plot of the first two
577 principal components from a GM analysis of 46 landmarks and 41 models. Axes not to
578 scale. Cranial reconstructions indicate shape changes (x200) along axes. Key: star,
579 unloaded model; squares, incisor bites; diamonds, premolar bites; triangles, M1 bites;
580 circles, M2 bites; plus signs, M3 bites; purple, model with all muscles; dark green, IOZM
581 removed; light green, ZM removed; blue, masseter removed; brown, posterior masseter
582 removed; red, temporalis removed; orange, medial pterygoid, removed; yellow, lateral
583 pterygoid removed.

Table 1(on next page)

Muscle forces applied to each side of the model.

PCSA and percentage activations of each muscle from Offermans & De Vree (1993).

Table 1. Muscle forces applied to each side of the model. PCSA and percentage activations of each muscle from Offermans & De Vree (1993).

	PCSA (cm^2)	Maximum force (N)	% activation		Applied force (N)	
			Incision	Mastication	Incision	Mastication
Masseter	2.886	86.58	20	70	17.32	60.61
Posterior masseter	0.654	19.62	0	40	0.00	7.85
ZM	3.360	100.80	60	100	60.48	100.80
IOZM	2.244	67.32	100	60	67.32	40.39
Temporalis	0.516	15.48	0	30	0.00	4.64
Medial pterygoid	1.130	33.90	15	90	5.09	30.51
Lateral pterygoid	0.519	15.57	60	70	9.34	10.90

Table 2(on next page)

Bite force, joint reaction force and mechanical advantage of each model.

Table 2. Bite force, joint reaction force and mechanical advantage of each model.

	All muscles	No masseter	No posterior masseter	No ZM	No IOZM	No temporalis	No medial pterygoid	No lateral pterygoid
Bite force								
I	154.6	138.3	154.3	122.5	49.9	154.3	152.0	154.3
PM	347.5	244.4	345.7	247.4	232.5	346.6	319.9	348.7
M1	395.6	279.0	393.5	280.7	265.7	394.6	362.5	397.4
M2	457.7	323.0	455.2	324.7	307.8	456.4	418.8	459.8
M3	539.6	380.8	536.7	382.9	362.7	538.1	494.1	541.9
Joint reaction force								
I	85.9	83.0	86.2	39.8	56.0	86.2	79.3	154.3
PM	2.8	29.2	3.4	-2.3	38.8	-0.4	-26.9	9.3
M1	-45.3	-5.4	-44.4	-35.7	5.5	-48.3	-69.6	-39.5
M2	-107.3	-49.4	-106.1	-79.7	-36.4	-110.2	-125.9	-102.0
M3	-189.2	-107.1	-187.5	-137.9	-91.3	-191.8	-201.1	-184.0
Mechanical advantage								
I	0.64	0.62	0.64	0.75	0.47	0.64	0.66	0.50
PM	0.99	0.89	0.99	1.01	0.86	1.00	1.09	0.97
M1	1.13	1.02	1.13	1.15	0.98	1.14	1.24	1.11
M2	1.31	1.18	1.30	1.33	1.13	1.32	1.43	1.28
M3	1.54	1.39	1.54	1.56	1.34	1.55	1.69	1.51

Figure 1

FE model showing muscle attachment sites and vectors.

Skull of *Pedetes capensis* shown in (A) lateral and (B) dorso-lateral view. Key: light green, IOZM; yellow, lateral pterygoid; blue, masseter; orange, medial pterygoid; brown, posterior masseter; red, temporalis; dark green, zygomaticomandibularis.

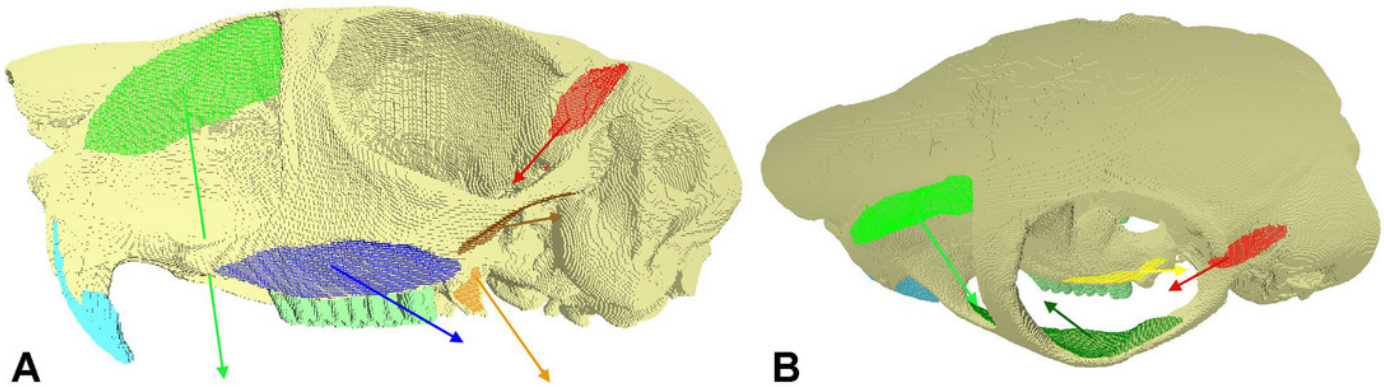

Figure 2

Landmarks used in GMM analysis of skull deformations.

Reconstruction of skull of *Pedetes capensis* in (A) dorsal, (B) ventral and (C) left lateral view. Landmarks 11-28 recorded on both sides of the skull. Landmark descriptions are given in Table S1.

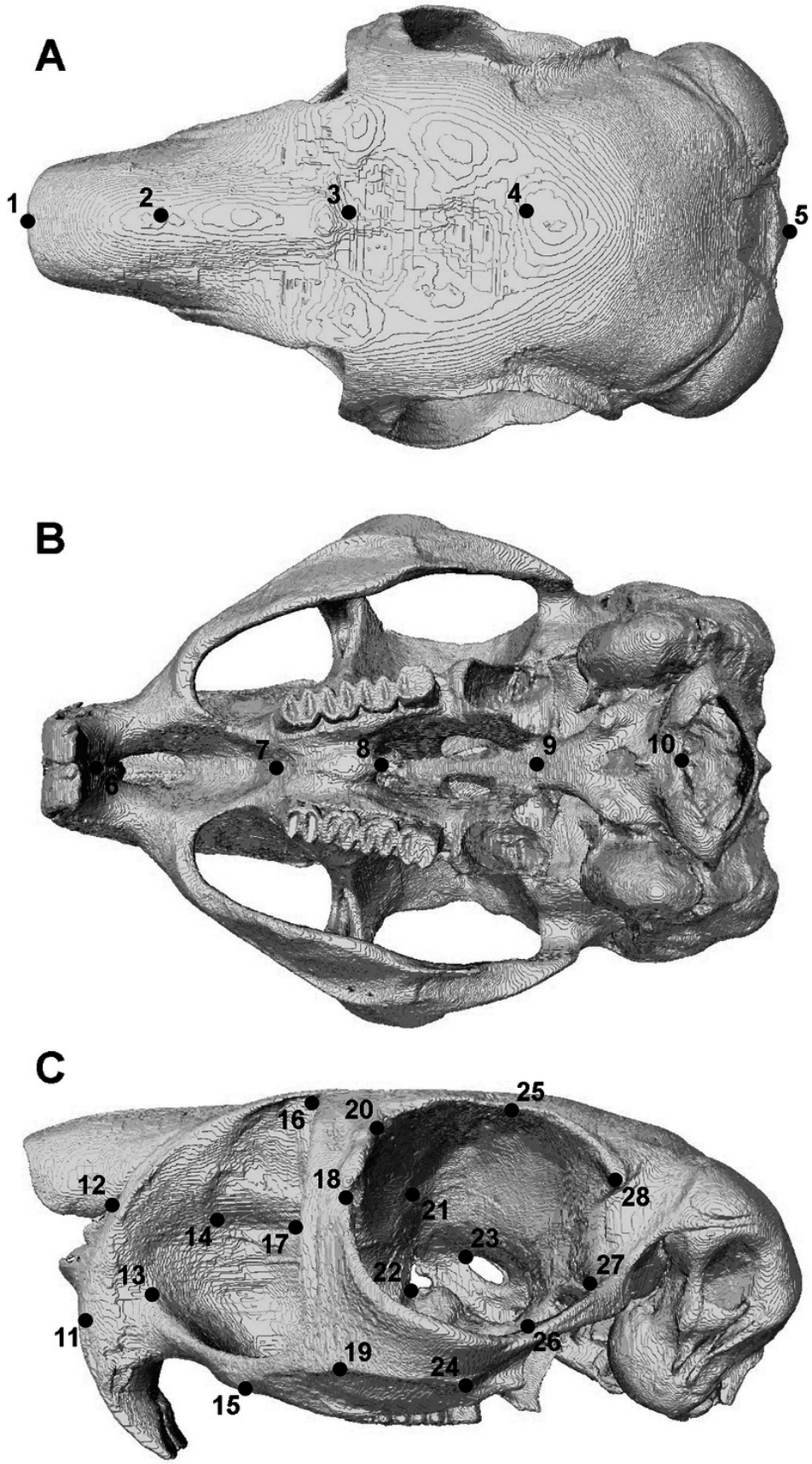
A
1
2
3
4
5
B
6
7
8
9
10
C
11
12
13
14
15
16
17
18
19
20
21
22
23
24
25
26
27
28

Figure 3

Mechanical advantage at each tooth predicted by FE model.

Abbreviations: I, incisor; PM, premolar; M1, first molar; M2, second molar; M3, third molar. Key: purple line with circle, model with all muscles; blue line with crosses, masseter removed; light green line with diamonds, IOZM removed; dark green line with triangles, ZM removed; orange line with squares, medial pterygoid removed. Models with posterior masseter, temporalis and lateral pterygoid removed not shown.

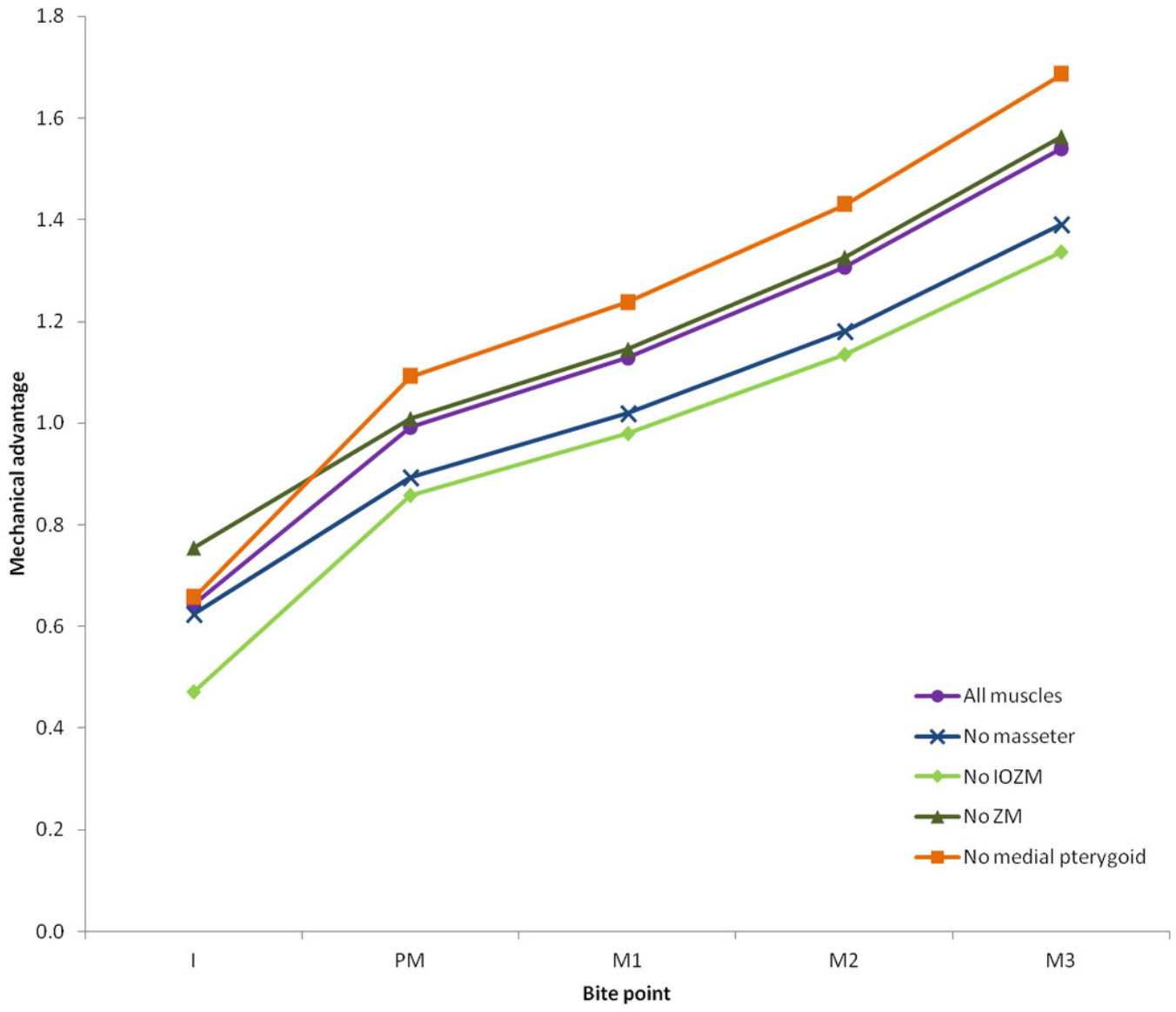

Figure 4

Predicted principal strains across the skull of *Pedetes capensis* during incisor and first molar biting.

Left, maximum (ε_1) principal strain; right, minimum (ε_3) principal strains. First line, model with all masticatory muscles included; second line, model with IOZM excluded; third line, model with masseter excluded; fourth line, model with ZM excluded.

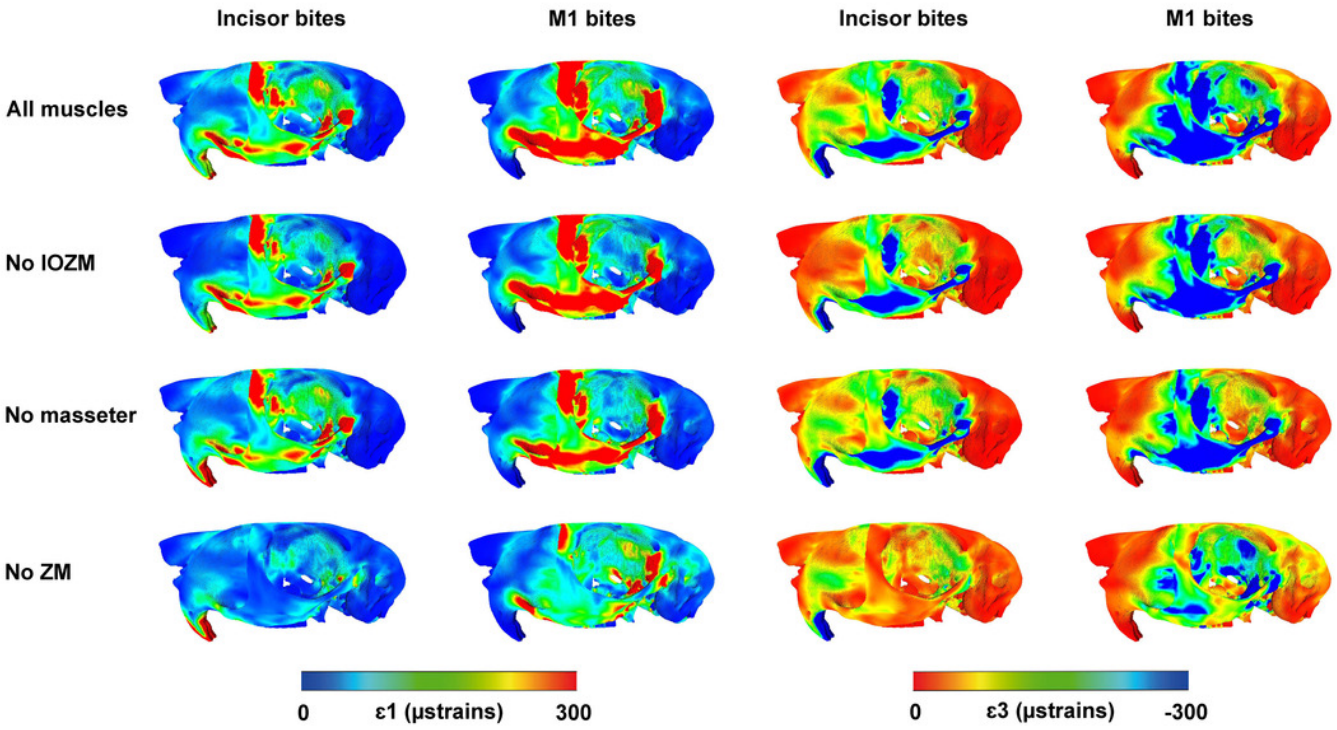

Figure 5

GM analysis of cranial deformations in *Pedetes capensis*.

Plot of the first two principal components from a GM analysis of 46 landmarks and 41 models. Axes not to scale. Cranial reconstructions indicate shape changes (x200) along axes. Key: star, unloaded model; squares, incisor bites; diamonds, premolar bites; triangles, M1 bites; circles, M2 bites; plus signs, M3 bites; purple, model with all muscles; dark green, lOZM removed; light green, ZM removed; blue, masseter removed; brown, posterior masseter removed; red, temporalis removed; orange, medial pterygoid, removed; yellow, lateral pterygoid removed.